

NASA TM-87336

NASA Technical Memorandum 87336

NASA-TM-87336 19860018145

Identification of Differences Between Finite Element Analysis and Experimental Vibration Data

Charles Lawrence
Lewis Research Center
Cleveland, Ohio

June 1986

LIBRARY COPY

JUL 24 1986

LANGLEY RESEARCH CENTER
LIBRARY, NASA
HAMPTON, VIRGINIA



NF01529

NASA

3 1176 01309 1955

IDENTIFICATION OF DIFFERENCES BETWEEN FINITE ELEMENT ANALYSIS
AND EXPERIMENTAL VIBRATION DATA

Charles Lawrence
National Aeronautics and Space Administration
Lewis Research Center
Cleveland, Ohio 44135

SUMMARY

E-3082

An important problem that has emerged from combined analytical/experimental investigations is the task of identifying and quantifying the differences between results predicted by F.E. analysis and results obtained from experiment. The objective of this study is to extend and evaluate the procedure developed by Sidhu for correlation of linear F.E. and modal test data to include structures with viscous damping. The desirability of developing this procedure is that the differences are identified in terms of physical mass, damping, and stiffness parameters instead of in terms of frequencies and modes shapes. Since the differences are computed in terms of physical parameters, locations of modeling problems can be directly identified in the F.E. model.

From simulated data it was determined that the accuracy of the computed differences increases as the number of experimentally measured modes included in the calculations is increased. When the number of experimental modes is at least equal to the number of translational degrees of freedom in the F.E. model both the location and magnitude of the differences can be computed very accurately. When the number of modes is less than this amount the location of the differences may be determined even though their magnitudes will be under estimated.

INTRODUCTION

The dynamic characteristics of structural systems are often predicted using Finite Element (F.E.) analysis and then later verified experimentally with dynamic analysis testing systems. Increased demands for reliability, minimal vibrations, optimum performance, and low cost design, among other criteria, have increased designers needs for sophisticated dynamic analysis testing techniques. Since the 1960's F.E. computer programs have become the preference of designers for analytical dynamic analysis. The use of F.E. computer codes has become especially widespread in the automotive and aerospace industries due to the requirement to analyze very large and complex structures. Commercial F.E. computer programs such as NASTRAN, ANSYS, and SAP (ref. 1) are available to anyone having access to a computer terminal.

In many situations experimental verification is required to insure the validity of the results predicted by the F.E. analysis. Aerospace structures, which are very expensive and have rigorous safety and reliability requirements normally require experimental verification (ref. 2). Automobile prototypes are also experimentally verified to insure that vibration and noise problems will not exist in production models. Hundreds of other applications of F.E. analysis and experimental validation can be found.

N86-27617 #

Digital signal analyzers are the most commonly used systems for experimental verification. Digital signal analyzers, which utilize the Fast Fourier Transform (FFT) developed in the 1960's (ref. 3), allow rapid and relatively accurate determination of structural transfer functions, resonant frequencies, and characteristic mode shapes. Modern digital analysis equipment has both automated the modal extraction process and decreased the required data acquisition and post-processing time. These systems have replaced traditional analog devices because of their high speed and their ability to measure many modes simultaneously.

An important problem that has emerged from these combined analytical/experimental investigations is the task of identifying and quantifying the differences between results predicted by F.E. analysis and results obtained from the experiment. Although both the F.E. and experimental methods can be accurate from a theoretical standpoint, inaccuracies do exist in their applications to real structural problems. In the case of F.E. modeling there is considerable uncertainty in the modeling of items such as boundary conditions, joint flexibilities, and damping. Because of this, the F.E. results are not exact since the input data itself is approximated. Also, it is not possible to completely eliminate experimental error. F.E. analysts take the responsibility for producing theoretically correct computer codes but sometimes do not place enough emphasis on predicting the behavior of real world structures. The experimentalist, through testing, often shows the limitations of the F.E. analysis, but do not always present clear cut procedures for quantifying the differences in a useful manner.

A communication gap can exist between the experimentalist and the F.E. analyst when the experimentalist can not provide the quantitative data required by the analyst to identify the differences between the experimental data and the F.E. model. The gap exists because the experimentalist normally measures frequencies and mode shapes in a vibration test, while the analyst requires a mass, damping, and stiffness matrix for describing the F.E. model.

It would be useful if the differences between the experimental data and F.E. model could be found in terms of discrete mass, stiffness, and damping. If this could be done, and the experimental data was reliable, a more accurate F.E. model with improved mass, damping, and stiffness descriptions could be created. This model could then be used for not only subsequent dynamic analysis, but also for static analysis, for studying the effects of structural modifications, or for any analysis requiring the use of a mass, damping, or stiffness matrix. It would be ideal if the discrete parameters could be measured experimentally but this is not practical. For example, to measure the values for a row or column in the stiffness matrix, a displacement would have to be applied to the real structure while every other degree of freedom was constrained, and then the forces at all the other degrees of freedom would need to be measured. This would be both time consuming and require elaborate fixtures and instrumentation. Experimental measurement of the mass and damping matrix would be at least equally complex, if not impossible.

One possible way to compare the experimental results to the F.E. model is to compute analytical frequencies and mode shapes from the F.E. equation of motion and then compare them to the frequencies and mode shapes obtained from the experiment. The limitation of making a comparison at this level is that

even though disagreements can be identified, the cause of the disagreements namely differences in the mass, damping, and stiffness matrices, can not be identified or quantified.

A more useful comparison between F.E. and experiment can be made through the equations of motion. By using the original F.E. equations and the equations of motion derived from the experimental data, differences between experiment and F.E. coefficients can be identified and corrected. Unfortunately, the procedure of deriving an equation of motion from the experimental frequencies and mode shapes is not straight forward. To derive the equation of motion from experimental data requires that the same number of modes as degrees of freedom in the F.E. model be experimentally measured and that the experimental data not contain any measurement error or noise. If both of these requirements are not met the experimental data can not be used to construct a correct equation of motion. Since the coefficients for the equations of motion are computed by inverting matrices containing the experimental mode shapes, these matrices must be square. In a typical experiment, the number of measured modes will not be equal to the number of degrees of freedom so the modal matrices will be rectangular instead of square. Another difficulty is that the experimental data will always contain some amount of experimental error and noise which makes the outcome of a matrix inversion questionable. Also, if the highest modes in the structure are not included in the experimental data the stiffness matrix computed from a modal matrix inversion will be incorrect (ref. 4). Finally, it is difficult to measure the values of the mode shapes corresponding to every degree of freedom used in the F.E. model. This causes the order of the experimental matrices to be less than those in the F.E. equations.

Previous research in this area has focused on using experimental data to improve F.E. models rather than on identifying the differences. Most of the techniques have been based on some form of a least squares fit. In the work by Berman and Flannelly (ref. 4), the analytical matrices are assumed to be close to the actual solution and then the smallest change in the analytical model that makes the experimental and analytical frequencies and mode shapes identical is found. This assumption will not necessarily lead to an analytical model that is physically representative of the actual structure. The only assurance is that the revised model will correctly predict the modes that were measured. The problems arising from using "incomplete" data (data containing fewer modes than there are in the F.E. model) are also discussed in this work. In reference 5, Fuh, Chen, and Berman use similar approaches for correcting structures with viscous damping.

Chen, Peretti, and Garba (ref. 6) refined a F.E. model of the Galileo spacecraft by first performing static tests to improve the stiffness matrix, and then dynamic tests for correcting the mass matrix. The mass matrix correction was based on a minimum change criteria. The limitations of this approach are that two independent sets of tests must be run, and again, there is no guarantee that actual physical characteristics will result from the least squares approach.

Hart and Yao (ref. 7) discuss the advantages of using weighted least squares and Bayesian estimation. By using these extended forms of least squares methods, uncertainties in both the experimental data and analytical model can be included in the updating procedure. It can be very important to define the uncertainty in the experimental data since this data often contains

more error than the F.E. description. It does not make much sense to attempt to improve a F.E. model with experimental data that is less certain than the F.E. model. By including relative uncertainties in the procedure, changes to the analytical model will not be applied indiscriminately and the possibility exists for retaining the physical meaning of the structure in the updated model.

Dobb, Blakely, and Gunday (ref. 8), and Blakely and Walton (ref. 9) applied the Bayesian estimation procedure to a F.E. model of an offshore platform and a dam. In their study the effects of change in the uncertainties in both the experimental data and the F.E. parameters were investigated. Unfortunately, well defined procedures do not exist for quantifying uncertainties so they had to be estimated using engineering judgement.

Sidhu (ref. 10) developed a procedure for approximating the difference between experimentally measured frequencies and mode shapes and F.E. parameters in terms of differences in mass, damping, and stiffness matrices. This approach has the potential for providing a direction to correct a F.E. model while retaining the physical characteristics of the real structure. The objective of this work is to extend the procedure developed by Sidhu for correlation of linear finite element and modal test data to include structures with viscous damping. In this study, the derivation of the extended procedure and several case studies which use simulated experimental data are presented. The purpose of developing this procedure is to formalize a process for identifying the differences between experimentally measured frequencies and mode shapes and F.E. models in terms of differences in mass, damping, and stiffness.

FORMULATION OF EQUATIONS

The free vibration equation of motion for a damped, linear system can be written as:

$$[M]\{\ddot{u}\} + [C]\{\dot{u}\} + [K]\{u\} = \{0\} \quad (1)$$

where $[M]$ is the mass matrix, $[C]$ is the viscous damping matrix, $[K]$ is the stiffness matrix, and $\{\ddot{u}\}$, $\{\dot{u}\}$, and $\{u\}$ are the acceleration, velocity, and displacement vectors, respectively. The size of $[M]$, $[C]$, and $[K]$ are $n \times n$ and $\{\ddot{u}\}$, $\{\dot{u}\}$, and $\{u\}$ are of size n , where n is the number of degrees of freedom in the equations of motion.

In only special cases can equation (1) be decoupled using normal modes (ref. 11). In general, when damping is present, the solution of this equation results in complex eigenvalues and eigenvectors appearing in conjugate pairs. Since there are pairs of roots there will be twice as many roots as there are displacement degrees of freedom and the modal matrix will be of the order $n \times 2n$ instead of $n \times n$. This rectangular modal matrix can not be used to decouple equation (1). Equation (1) can be rewritten in state vector form as:

$$[A]\{\dot{y}\} + [B]\{y\} = \{0\} \quad (2)$$

$$\text{where } \{y\} = \begin{Bmatrix} \{\dot{u}\} \\ \{u\} \end{Bmatrix} \quad [A] = \begin{bmatrix} [0] & [M] \\ [M] & [C] \end{bmatrix} \quad [B] = \begin{bmatrix} -[M] & [0] \\ [0] & [K] \end{bmatrix}$$

([A] and [B] are of order $2n \times 2n$ and $\{y\}$ is of order $2n$.)

The advantage of writing the equation of motion in state vector form is that the modal matrix can now be used to decouple the equation. Assuming a solution $\{y\} = \{\Phi\}e^{st}$ and substituting into equation (2) leads to the eigenvalue problem:

$$\{[A]s + [B]\}\{\Phi\} = \{0\} \quad (3)$$

For less than critical damping, the solution of this equation yields $2n$ complex eigenvalues s_r , where $s_r = -w_r \zeta_r \pm i w_{Dr}$. w_r is the natural frequency, w_{Dr} is the damped natural frequency, and ζ_r is the damping ratio for mode r . An equal number of complex eigenvectors are also obtained.

Substituting the modal matrix $[\Phi]$ into equation (3) and premultiplying by $[\Phi]^T$ leads to:

$$[\Phi]^T[A][\Phi][\backslash s \backslash] + [\Phi]^T[B][\Phi] = \{0\} \quad (4)$$

from orthogonality

$$[\Phi]^T[A][\Phi] = [\backslash a \backslash] \quad \text{and} \quad [\Phi]^T[B][\Phi] = [\backslash b \backslash]$$

where $[\backslash a \backslash]$ and $[\backslash b \backslash]$ are diagonal matrices.

If the eigenvectors are normalized with respect to the [A] matrix then:

$$[\Phi]^T[A][\Phi] = [I] \quad (5)$$

and

$$[\Phi]^T[B][\Phi] = -[\backslash s \backslash] \quad (6)$$

Since the objective is to determine the differences between the experimental model and the analytical model we need to find a common ground that will allow the comparison of the structural matrices computed from the F.E. analysis to the experimental frequencies and mode shapes. The differences between the F.E. "[B]" matrix and the [B] matrix computed from the experimental data (assuming that a [B] matrix can be created from the experimental data) is written as:

$$[D]_B = [B]_{\text{exp}} - [B]_{\text{F.E.}} \quad (7)$$

rearranging

$$[B]_{\text{exp}} = [B]_{\text{F.E.}} + [D]_B$$

then inverting both sides

$$[B]_{\text{exp}}^{-1} = \{[B]_{\text{F.E.}} + [D]_B\}^{-1}$$

and factoring out $[B]_{\text{F.E.}}$

$$[B]_{\text{exp}}^{-1} = \{[B]_{\text{F.E.}} \{[I] + [B]_{\text{F.E.}}^{-1} [D]_B\}\}^{-1}$$

and

$$[B]_{\text{exp}}^{-1} = \{[I] + [B]_{\text{F.E.}}^{-1} [D]_B\}^{-1} [B]_{\text{F.E.}}^{-1} \quad (8)$$

If the bracketed expression in equation (8) is expanded using a Taylor series (refs. 12 and 13) and terms past the first derivative are dropped, equation (8) can be approximated by:

$$[B]_{\text{exp}}^{-1} \approx \{[I] - [B]_{\text{F.E.}}^{-1} [D]_B\} [B]_{\text{F.E.}}^{-1}$$

multiplying out $[B]_{\text{F.E.}}^{-1}$

$$[B]_{\text{exp}}^{-1} \approx [B]_{\text{F.E.}}^{-1} - [B]_{\text{F.E.}}^{-1} [D]_B [B]_{\text{F.E.}}^{-1}$$

and then rearranging

$$-[B]_{\text{exp}}^{-1} + [B]_{\text{F.E.}}^{-1} \approx [B]_{\text{F.E.}}^{-1} [D]_B [B]_{\text{F.E.}}^{-1}$$

and solving for $[D]_B$

$$[D]_B \approx [B]_{\text{F.E.}} \{[B]_{\text{F.E.}}^{-1} - [B]_{\text{exp}}^{-1}\} [B]_{\text{F.E.}} \quad (10)$$

Using equation (6) to obtain $[B]_{\text{F.E.}}^{-1}$ and substituting into equation (10) the final expression for the difference matrix $[D]_B$ is obtained:

$$[D]_B \approx [B]_{\text{F.E.}} \{[\Phi]_{\text{F.E.}} [\backslash s \backslash]_{\text{F.E.}}^{-1} [\Phi]_{\text{F.E.}}^T - [\Phi]_{\text{exp}} [\backslash s \backslash]_{\text{exp}}^{-1} [\Phi]_{\text{exp}}^T\} [B]_{\text{F.E.}} \quad (11)$$

The same approach can be used for deriving the difference in the $[A]$ matrix. In this case:

$$[D]_A \approx [A]_{\text{F.E.}} \{[\Phi]_{\text{F.E.}} [\Phi]_{\text{F.E.}}^T - [\Phi]_{\text{exp}} [\Phi]_{\text{exp}}^T\} [A]_{\text{F.E.}} \quad (12)$$

The format of equations (11) and (12) are well suited for computing the differences between the F.E. model and experimental data. Since these equations do not require any inversion of the modal matrices, the fact that all the modes are not measured does not cause a problem. As discussed previously, the modal matrix will not be completely known since fewer modes than degrees of freedom are typically measured. An inversion of the frequency matrices are required, but this does not present any problems since these matrices are diagonal and their inverses are just the reciprocal of the diagonal terms.

Once $[D]_A$ and $[D]_B$ are computed, the disagreement between the F.E. and experimental descriptions of the structure can be found. Since there is a direct relationship between the elements of the mass, damping, and stiffness matrices and the elements of the $[A]$ and $[B]$ matrices, the discrepancies in mass, damping, and stiffness at any degree of freedom in the structure can be found by merely picking out values from the $[D]_A$ and $[D]_B$ matrices. For example, the disagreement in damping at the first degree of freedom would be obtained from the $[D]_A$ matrix at location $[D(n+1, n+1)]_A$, the mass disagreement at $[D(1, n+1)]_A$, and the stiffness disagreement at $[D(n+1, n+1)]_B$. Note that the mass discrepancy can be found from either one of two partitions in the $[D]_A$ matrix or the $[D]_B$ matrix.

It was mentioned previously that in preactive experimental mode shape data will normally not be available at all of the degrees of freedom used in the F.E. model. When this situation exists, either the mode shape data must be interpolated (ref. 7) or the F.E. model reduced (ref. 16). In this paper it will be assumed that one of these procedures has already been applied, thus rendering the number of degrees of freedom equal to the number of experimental measurement points where mode shape data is taken. It will also be assumed that the experimental mode shapes are measured at the F.E. node locations.

Sample Problem One

Sample problem one consists of a planar cantilever beam. Two finite element models were used in the analysis. This first model, referred to as the analytical model, is used for computing the frequencies and mode shapes that would normally be generated by an analytical analysis. The second model, referred to as the "experimental" model, is used for simulating frequencies and mode shapes that would be obtained by performing an actual experimental modal analysis on a real beam. It is advantageous to use simulated data in place of real data because the property matrices corresponding to the simulated data are known, whereas the property matrices for any real structure are unknown. Since the mass, damping, and stiffness matrix are known for the simulated experimental data, the exact error matrices can be compared to the error matrices generated by the equations derived in this study and the procedures can be evaluated.

The analytical model is made up of nine, equally spaced node points and eight connecting beam elements (fig. 1). All of the degrees of freedom are constrained at node 1 and every degree of freedom except for the z-displacement and y-rotation are constrained at the other node points. This leaves sixteen active degrees of freedom for the structure. The section properties for the beam elements are 2.6×10^{-3} for the moment of inertia, 10×10^6 for Young's modulus, and 2.6×10^{-4} for the mass density per unit length.

The complex eigenvalue extraction solution sequence (Solution 28) of the MSC/NASTRAN finite element program was used to compute the free vibration frequencies and mode shapes for the beam. The Hess method (ref. 14) was selected for extracting the modes since this method is more efficient when all of the modes are desired. All of the modes were initially required for a complete verification of the difference matrix routines.

The simulated experimental model was made to differ from the F.E. model by adding a concentrated mass, damper, and spring to the beam. The location of these elements is shown in figure 1. The values used for the elements are listed in table I as ΔM , ΔC , and ΔK . The mass, damping, and stiffness from the F.E. model at the same nodes and directions are also listed to give an indication of the relative magnitude of the differences. NASTRAN was again used for computing the complex frequencies and mode shapes of the experimental model.

Table II shows the comparison between the computed eigenvalues for the analytical model and the simulated experimental model for each of the four cases. All 16 of the modes were computed by NASTRAN. From table II, a comparison can be made between the complex valued eigenvalues. As expected, the real part of the analytical eigenvalues are zero since there is no damping present in the F.E. model, and the real part of the experimental eigenvalues are non-zero since damping is present. In general, the addition of the tip mass and the damper tends to lower the frequencies while the spring raises the frequencies. The modal damping is totally dependent on the concentrated damper.

The imaginary (frequency) part of the F.E. and experimental eigenvalues are plotted in figure 3 for case 1. If the eigenvalues matched exactly they would plot directly on the straight, 45° line. There is a small deviation from the straight line, but not enough to indicate any significant differences between the analytical and experimental models. Even if there were large deviations between the analytical and experimental eigenvalues, there would not be any way to use the results in figure 3 or table II to relate the deviations to differences in physical mass, damping, or stiffness coefficients.

The real components of the first four mode shapes for the analytical model (case 1) are plotted in figure 4. Only the translational degrees of freedom are plotted. Even though the first frequency has the largest deviation (figure 3) the first mode shape matches up very closely. The opposite occurs for the second and third modes where the mode shapes deviate from each other while the frequencies are very similar. As with the frequency plots, there is no way to relate the deviation from perfect correlation in mode shape plots to physical differences in mass, damping, or stiffness.

The Difference Matrix program was used to relate the differences between the experimental and analytical models in terms of differences in mass, damping, and stiffness. The computer program was verified using all four cases and various numbers of modes as input data. When all of the modes are included as input the only approximation in the procedure is from the Taylor series truncation. As previously discussed, in a real situation all the modes would not be available from tests. Plots of mass, damping, and stiffness difference matrices for case 1, using all 16 modes are shown in figure 4. The differences are plotted on a grid where each intersection of a grid line corresponds to a location in the matrix being plotted. For example, the mass difference shown in the figure corresponds to the (15, 15) location in the structure's mass matrix. In the figure the physical differences between the analytical and experimental models are clearly defined. The mass difference matrix indicates a mass difference at degree of freedom 15 which corresponds to the translational direction at the beam tip where the concentrated mass was added. The damping and stiffness errors at degree of freedom seven and one respectively, correspond to the locations of the concentrated damper and spring. There

were no other differences between the analytical and experimental models which is indicated by the flat areas in all three of the difference matrix plots. Even though the location of the difference is exact, there is some amount of disagreement between the actual magnitudes of the mass and stiffness, and the magnitudes computed by the error matrix program. The program computed a mass difference of 0.00011 while the actual concentrated mass was 0.0002. The spring magnitude was computed to be 3294, while the real spring was 5000. The magnitudes of the actual damper and the magnitude computed by the program were both 1.0. It is not surprising that the computed mass differences was so far off since the mass added to the experimental model was almost as great as the original mass in the analytical model. Since all of the modes were included in these calculations, the differences between the real values and the computed ones can be attributed to the higher order terms that are missing in the Taylor expansion. A procedure for improving the accuracy of the magnitudes will be discussed later in this section.

When less than all 16 modes are included in the calculations the results deteriorate. In figure 5 results are shown for the case where only one mode was included as input into the Difference Matrix program. The mass and damping difference plots do not show anything but some distributed noise. The stiffness difference plot indicates a difference at the spring location, but the difference is of the wrong magnitude. (After examining the data, the sign of the difference was also found to be incorrect) Figure 6 shows difference plots where 10 modes are included as input. In this case the noise has virtually disappeared and the correct locations of the differences have shown up.

A compilation of results for all four test cases are shown in figures 7 to 9. In these figures the ratio of the computed to actual difference at the mass, damper, and spring location are plotted as a function of the number of modes used as input data into the Difference program. All four cases were run using 16, 8, 5, 3, 2, and 1 modes as input into the Difference program. From the mass difference plot (fig. 7), it is seen that when the mass difference is large (case 1), the computed difference is only about half of the correct difference. When the mass difference was reduced (cases 2, 3 and 4) the computed difference was much closer to the correct difference. If the mass difference is as great or greater than the analytical mass, the location of the difference will be correct but the magnitude will not. From cases 2, to 4 it is also seen that the computed mass difference does not change with the level of the damping or stiffness differences.

Figure 8 shows the computed damping differences for the four cases. This plot shows that the differences are independent of the level of damping as well as independent of the magnitude of the mass and stiffness difference. Even when large amounts of damping are present in the structure the damping calculations are accurate (the damping level in case 2 was close to critical). It is encouraging to note that the accuracy is independent of the damping difference level, because in analytical modeling it is the damping values that are the most difficult to predict. Thus for a typical structure the difference procedure would work fairly well, since the mass and stiffness differences would ordinarily be small, and the magnitude of the damping difference would not matter.

Figure 9 shows the effects of the various difference ratios on the computed stiffness differences. Similar to the mass calculations, the accuracy of the difference is dependent upon its relative magnitude. When the stiffness difference is relatively large, the computed difference is inaccurate; when the difference is small, the computed value is much closer to the actual value. Again, the computed difference is independent of the level of the differences in the other parameters.

From any of the figures presented thus far it is apparent that when only a few modes are included the results are meaningless. When less than eight modes are included the results are poor, and past eight modes the results are good and do not improve by including more than the first eight modes. To determine how the number of degrees of freedom used in the model effects the number of modes required for good results, a new model of the cantilever beam was constructed using 32 degree of freedom instead of 16.

The difference plots for this model were computed using the differences from case 3. The results are shown in figure 10. The difference matrices using 16 modes as input are shown in figure 11. From these results it is seen that while only 8 modes produced good results in the 16 degree of freedom model, at least 16 modes are needed in the 32 degree of freedom model.

Previously, it has been shown that the accuracy of the computed differences are dependent on the magnitude of the differences and the number of modes included in the calculations. In an attempt to improve the accuracy an iterative procedure was implemented (fig. 12). In this procedure the differences computed by the Difference program are accumulated from all previous iterations and are then added to the mass, damping, and stiffness matrices for the analytical model. The updated analytical model is then used to compute a new set of differences for the next iteration.

The iterative procedure was tested using the differences from test case 3 and the sixteen degree of freedom model. The results for three iterations are shown in figure 13. Without iterating, it was shown that when all sixteen modes are included in the calculations the results are very good. After iterating only twice, the results are exact. The same is also true when only eight modes are used. In general, when less than eight modes are used, the accuracy of the computed differences are not improved significantly by iterating. When only a few modes are included, the accuracy is not improved at all. The advantage of using the iteration procedure is that when an adequate number of modes are used the results will converge to the exact values regardless of the magnitude of the differences. The limitation of the iterative process is that it does not reduce the number of modes required for good results.

SAMPLE PROBLEM TWO

The second sample problem consists of a planar, simply supported beam. The finite element model of this problem is made up of nine node points and eight connecting beam elements (fig. 14). All of the degrees of freedom are constrained, except for the y-rotations at nodes one to nine, and the z-translations at nodes two through eight. There are sixteen degrees of

freedom for this problem. The same section properties that were used of for the first sample problem are also used here. The difference matrix plots for this problem were generated using the iteration scheme shown in figure 16.

The "experimental" model was made to differ from the analytical model by adding three concentrated springs and seven dampers to the beam model. The locations and properties for these elements are shown in the figure. This sample problem differs from the first one in that the differences in the first problem were limited to a single mass, damper, and spring, while in this problem there are several springs and dampers at every node. Also, the level of damping is much less in this problem than in the previous one.

A comparison of the eigenvalues for the second sample problem is shown in table III. From this comparison it is seen that the major differences between the analytical and experimental models are in the first frequency and the modal damping in the first seven modes. Beyond the seventh mode there are not any differences between the analytical and experimental eigenvalues. The first frequency is higher for the experimental model because of the additional stiffness from the three springs. The modal damping is different because the experimental model has the seven translational dampers while the analytical model does not have any damping. It is understandable that there is no modal damping in the higher modes for the experimental model since the higher modes are dominated by rotations and the dampers only act in the translation direction.

The computed damping and stiffness difference matrices using the first mode only as input into the Difference program are shown in figure 15. From these plots it is impossible to identify any of the differences that actually exist between the analytical and experimental models. When only one mode was used for the first sample problem calculations the differences could not be identified either. When the number of modes was increased to four (fig. 16) the correct differences were reasonably apparent in the difference plots. For the stiffness matrix plot, differences appear at degree of freedom 4, 6, and 8 which corresponds to the locations of the three springs that were added to the experimental model. In addition to the differences at these degrees of freedom, differences also appear at some of the other degrees of freedom. These differences do not actually exist in the models and would not appear if more modes were used as input. Many of these "extra" differences can be eliminated by examining the possible coupling that may exist in the analytical mode. For example, node two and six are not connected to each other so degrees of freedom 2 (z-translation, node two) and degree of freedom 10 (z-translation, node six) are uncoupled which allows for location (2,10) and (10,2) in the difference matrix to be set to zero. The same logic can be used to eliminate some of the other unobtainable differences appearing in the plots.

In figure 17, the difference plots using four modes are recreated, except that the differences at uncoupled degrees of freedom are set to zero. In these plots the correct differences are even more evident although some differences continue to appear where there are not any true differences. There does not appear to be any way to eliminate these "extra" differences except by using more modes in the calculations. When the number of modes is increased to six (fig. 18), both the computed stiffness and damping difference matrices are very accurate. In addition, no significant differences appear where they do not actually exist in the models. In figure 19, plots are shown where all sixteen modes are included in the computations, and as expected, the results are almost exact.

CONCLUSION

A general procedure for identifying and quantifying the differences between F.E. models and experimental data has been developed and demonstrated with simulated experimental data. The differences, which can be computed for linear, viscously damped structures, are presented in terms of mass, damping, and stiffness coefficients. Since the differences are computed in terms of mass, damping, and stiffness coefficients, possible modeling problems can be identified in the F.E. or analytical model.

From data generated for a damped cantilever beam and a damped simply supported beam, it was determined that the accuracy of the computed differences increases as the number of experimentally measured modes included in the calculations is increased. When the number of experimental modes is at least equal to the number of translational degrees of freedom both the location and magnitude of the differences can be computed very accurately. When the number of modes is less than this amount the location of the differences may be determined even though their magnitudes will be under estimated. When too few modes are available neither the location or the magnitudes of the differences can be identified.

In practice, it will be required to measure the experimental frequencies and mode shapes very accurately before the differences can be attributed to shortcomings in the analytical model. If the experimental data is not precise, the computed differences can still provide considerable insight into the possible locations of deficiencies. The difference is that the deficiencies may be in the experiment and some judgement will be required to decide whether to modify the experiment or the analytical model.

REFERENCES

1. Schaeffer, H.G.: A Review of the International Symposium on Structural Mechanics Software. Comput. Struct., vol. 8, no. 5, 1978, pp. 589-598.
2. Modal Analysis Verifies Satellite's Structural Math Model. Design News, vol. 41, no. 3, Feb. 4, 1985, pp. 86-90.
3. Cooley, J.W.; and Tukey, J.W.: An Algorithm for the Machine Calculation of Complex Fourier Series. Mathematics of Computation, vol. 19, 1965, pp. 297-301.
4. Berman, A.; and Flannelly, W.G.: Theory of Incomplete Models of Dynamic Structures. AIAA J., vol. 9, no. 8, Aug. 1971, pp. 1481-1487.
5. Fuh, J.S.; Chen, S.Y.; and Berman, A.: System Identification of Analytical Models of Damped Structures. 25th Structures, Structural Dynamics and Materials Conference, Pt. 2, AIAA, 1984, pp. 112-116.
6. Chen, J.C.; Peretti, L.F.; and Garba, J.A.: Spacecraft Structural System Identification by Modal Test. 25th Structures, Structural Dynamics, and Materials Conference, Pt. 2, AIAA, 1984, pp. 478-489.

7. Hart, G.C.; and Yao, J.T.P.: System Identification in Structural Dynamics. ASCE J. Eng. Mech. Div., vol. 103, no. 6, Dec. 1977, pp. 1089-1104.
8. Dobbs, M.W.; Blakely, K.D.; and Gundy, W.E.: System Identification of Large-Scale Structures. SAE Paper 811050, Oct. 1981.
9. Blakely, K.D.; and Walton, W.D.: Selection of Measurement and parameter Uncertainties for Finite Element Model Revision. Proceedings of the 2nd International Modal Analysis Conference and Exhibit, vol. 1, P.B. Juhl and D.J. Demichele, eds., Union College Graduate Continuing Studies, Schenectady, NY, 1984, pp. 82-88.
10. Sidhu, J.: Reconciliation of Predicted and Measured Modal Properties of Structures. PhD Dissertation, Department of Mechanical Engineering, Imperial College of Science and Technology, London, 1983.
11. Meirovitch, L.: Analytical Methods in Vibrations. MacMillan, 1967.
12. Frazer, R.A.; Duncan, W.J.; and Collar, A.R.: Elementary Matrices and Some Applications to Dynamics and Differential Equations. Cambridge University Press, 1960.
13. Thomas, G.B. Jr.: Calculus and Analytic Geometry. 4th ed., Addison-Wesley, 1972.
14. The NASTRAN Theoretical Manual. NASA SP-221 (06), Jan. 1981.

TABLE I. - TEST CASES FOR
SAMPLE PROBLEM ONE

Case	$\Delta M/M^a$	$\Delta C/C^b$	$\Delta k/k^c$
1	$\frac{2 \times 10^{-4}}{2.6 \times 10^{-4}}$	$\frac{1.0}{0}$	$\frac{5000}{78000}$
2	$\frac{5 \times 10^{-5}}{2.6 \times 10^{-4}}$	$\frac{1.8}{0}$	$\frac{2500}{78000}$
3	$\frac{5 \times 10^{-5}}{2.6 \times 10^{-4}}$	$\frac{1.8}{0}$	$\frac{2500}{78000}$
4	$\frac{5 \times 10^{-5}}{2.6 \times 10^{-4}}$	$\frac{1.0}{0}$	$\frac{25000}{78000}$

^aRatio of mass Δ to F.E.
mass at node 9.

^bRatio of damping Δ to F.E.
damping at node 5.

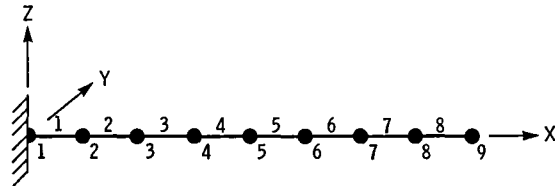
^cRatio of stiffness Δ to
F.E. stiffness at node 2.

TABLE II. - COMPARISON OF ANALYTICAL AND "EXPERIMENTAL" EIGENVALUES FOR SAMPLE PROBLEM ONE

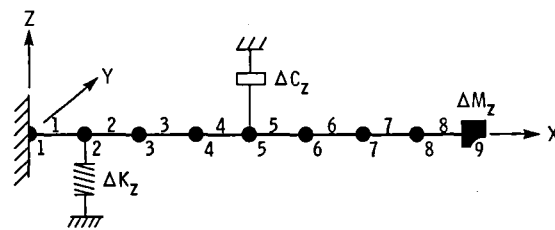
Mode	Analytical eigenvalue	Case 1	Case 2	Case 3	Case 4
		Experimental eigenvalue	Experimental eigenvalue	Experimental eigenvalue	Experimental eigenvalue
1	0 + 1371	-44.3 + 1301	-123 + 1111	-53 + 1331	-45 + 1501
2	0 + 8401	-247 + 7611	-438 + 5811	-245 + 7821	-258 + 8741
3	0 + 2 3121	-179 + 2 2711	-12 + 2 3141	-74 + 2 3171	-31 + 2 5251
4	0 + 4 4471	-203.9 + 4 3811	-378 + 4 3591	-21.4 + 4 4251	-183 + 4 7941
5	0 + 7 1971	-28.2 + 7 1781	-30 + 7 2031	-17 + 7 2071	-59 + 7 6921
6	0 + 10 4271	-195 + 10 4281	-360 + 10 3871	-202 + 10 4301	-158 + 10 9721
7	0 + 13 7571	-247 + 13 7941	-35 + 13 7761	-19.6 + 13 7801	-55 + 14 2351
8	0 + 16 3711	-197 + 16 3691	-359 + 16 3041	-199 + 16 3591	-168 + 16 5721
9	0 + 63 0171	0 + 62 9221	0 + 62 9821	0 + 62 9821	0 + 62 9821
10	0 + 75 7271	0 + 75 7111	0 + 75 7211	0 + 75 7211	0 + 75 7211
11	0 + 84 0331	-3 + 83 9441	-5 + 84 0191	-3 + 84 0191	-3 + 84 0191
12	0 + 94 0261	0 + 93 9741	0 + 94 0071	0 + 94 0071	0 + 94 0071
13	0 + 103 9281	-2 + 103 8751	-4 + 103 9091	-2 + 103 9091	-2 + 103 9091
14	0 + 112 5991	0 + 112 5591	0 + 112 5841	0 + 112 5841	0 + 112 5841
15	0 + 119 2781	0 + 119 2561	-1 + 119 2701	0 + 119 2701	0 + 119 2701
16	0 + 123 4711	0 + 123 4661	0 + 123 4701	0 + 123 4691	0 + 123 4701

TABLE III. - COMPARISON OF
ANALYTICAL AND
"EXPERIMENTAL"
EIGENVALUES
FOR SAMPLE
PROBLEM
TWO

Mode	Analytical eigenvalue	Experimental eigenvalue
1	0 + 3861	-48 + 4881
2	0 + 1 5411	-48 + 1 5601
3	0 + 3 4551	-48 + 3 4661
4	0 + 6 0931	-48 + 6 0951
5	0 + 9 3491	-47 + 9 3521
6	0 + 12 9171	-47 + 12 9191
7	0 + 16 0311	-48 + 16 0331
8	0 + 62 6681	0 + 62 6681
9	0 + 62 9301	0 + 62 9301
10	0 + 76 6171	0 + 76 6171
11	0 + 85 5771	0 + 85 5771
12	0 + 95 5621	0 + 95 5621
13	0 + 105 1191	0 + 105 1191
14	0 + 113 3471	0 + 113 3471
15	0 + 119 6331	0 + 119 6331
16	0 + 123 5631	0 + 123 5631



(a) Analytical model.



(b) "Experimental" model.

Figure 1. - Sample problem one.

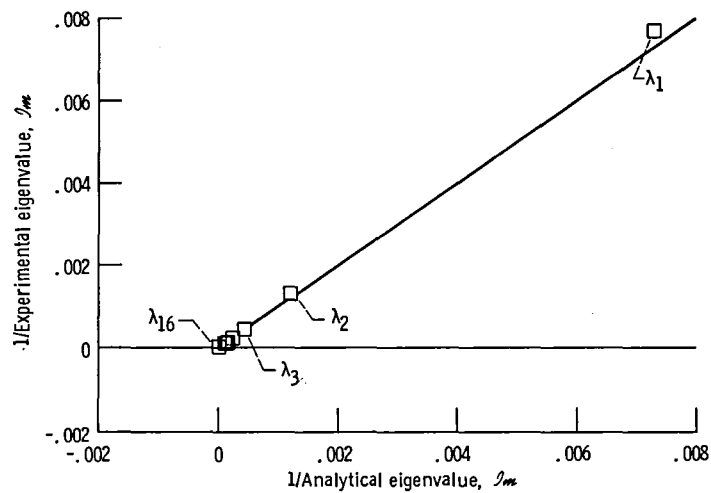


Figure 2. - Comparison of frequency data for sample problem one, case 1.

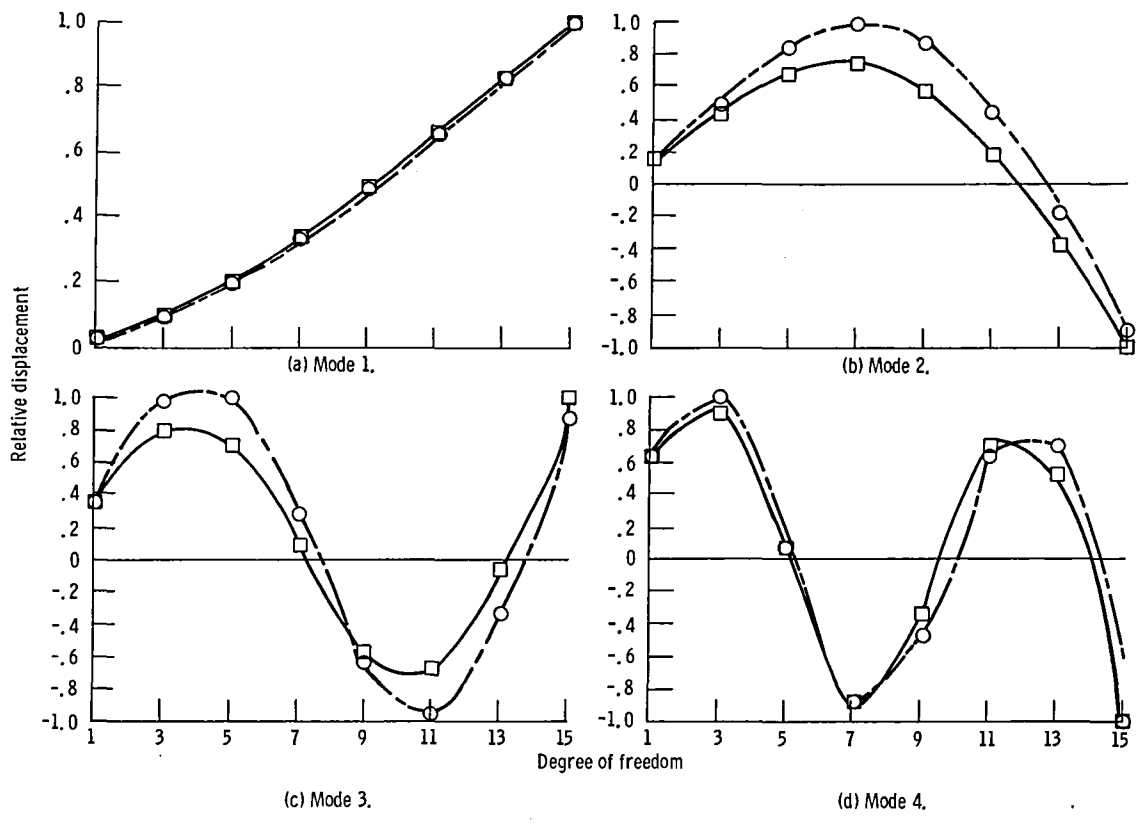
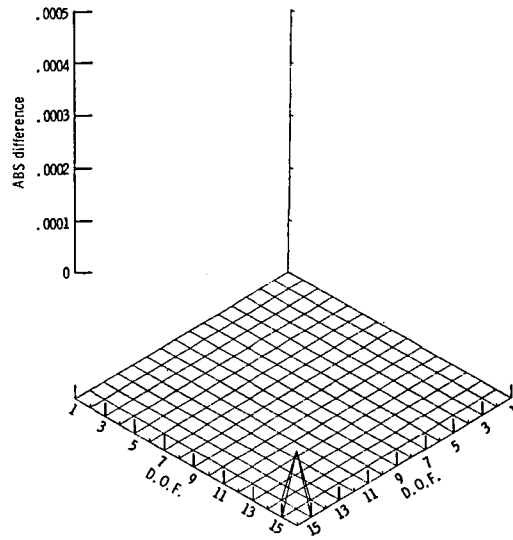
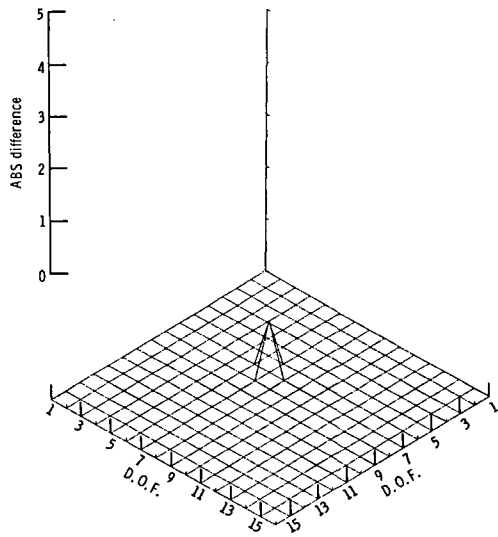


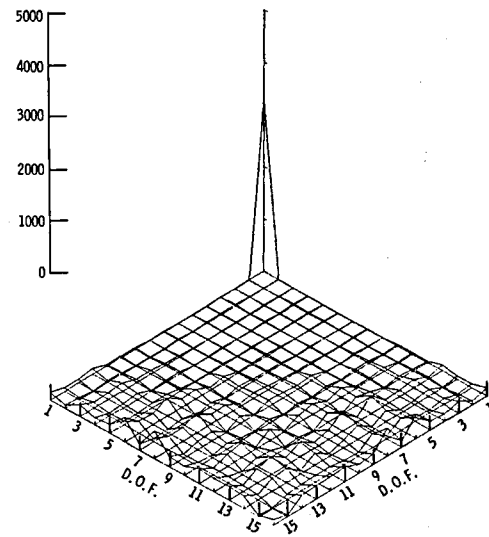
Figure 3. - Comparison of mode shapes for sample problem one, case 1.



(a) Mass difference matrix.

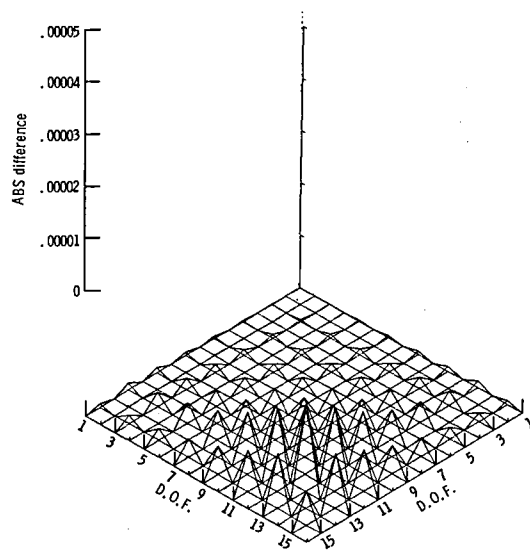


(b) Damping difference matrix.

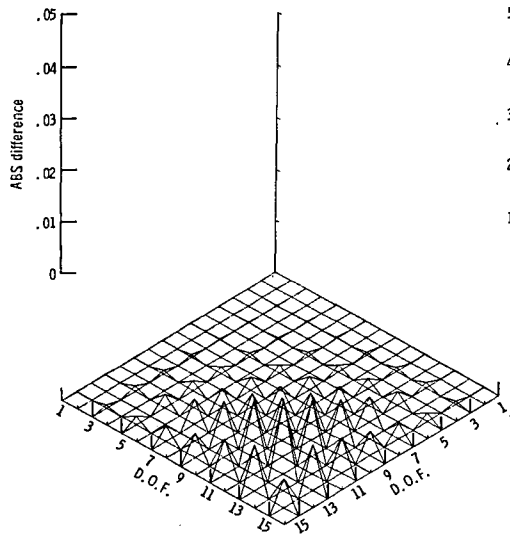


(c) Stiffness difference matrix.

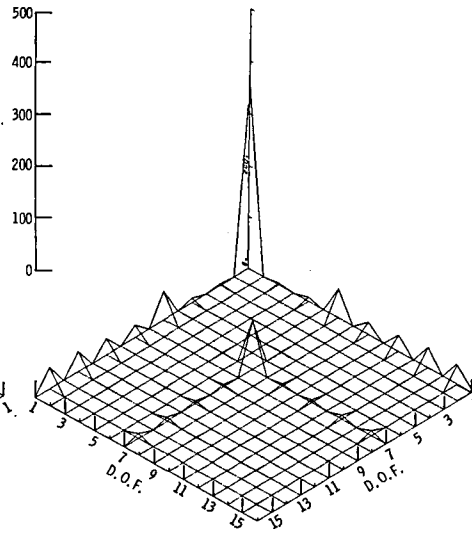
Figure 4. - Computed differences for sample problem one, case 1, using 16 modes.



(a) Mass difference matrix.

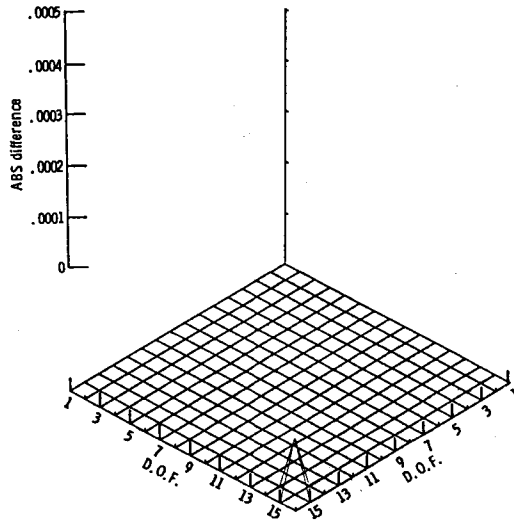


(b) Damping difference matrix.

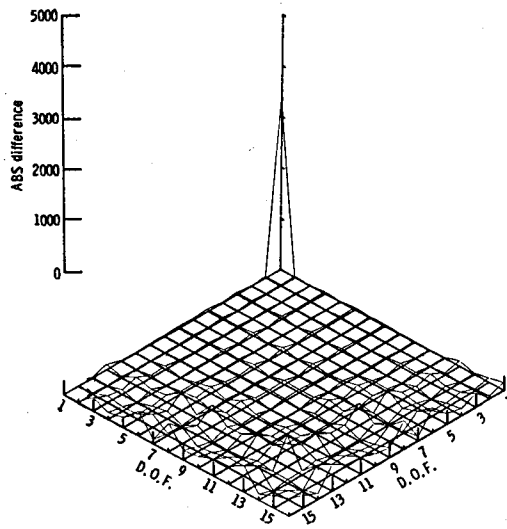


(c) Stiffness difference matrix.

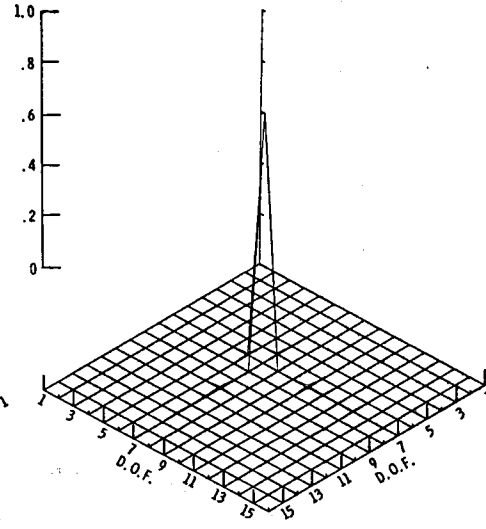
Figure 5. - Computed differences for sample problem one, case 1, using 1 mode.



(a) Mass difference matrix.



(b) Stiffness difference matrix.



(c) Damping difference matrix.

Figure 6. - Computed differences for sample problem one, case 1, using 10 modes.

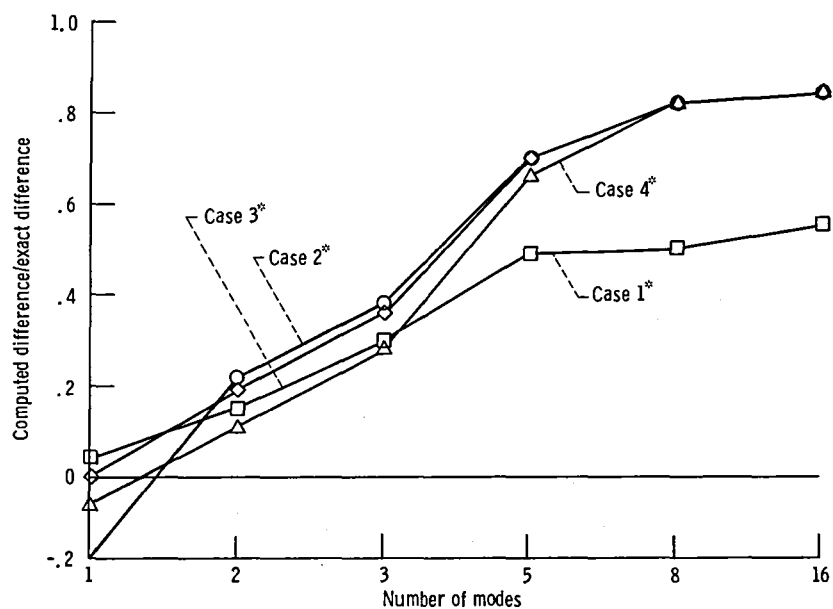


Figure 7. - Mass difference at concentrated mass location (sample problem one). (*See table I for case definition.)

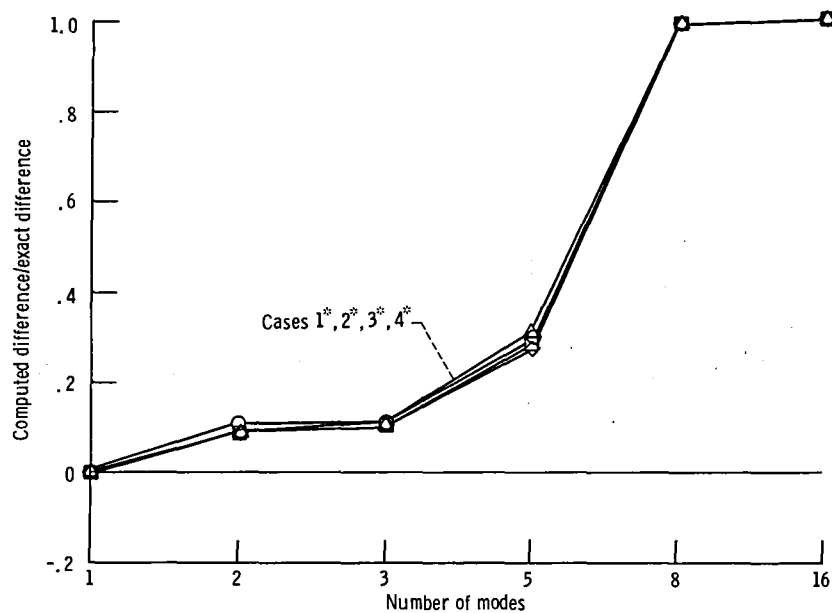


Figure 8. - Damping difference at concentrated damper location (sample problem one). (*See table I for case definition.)

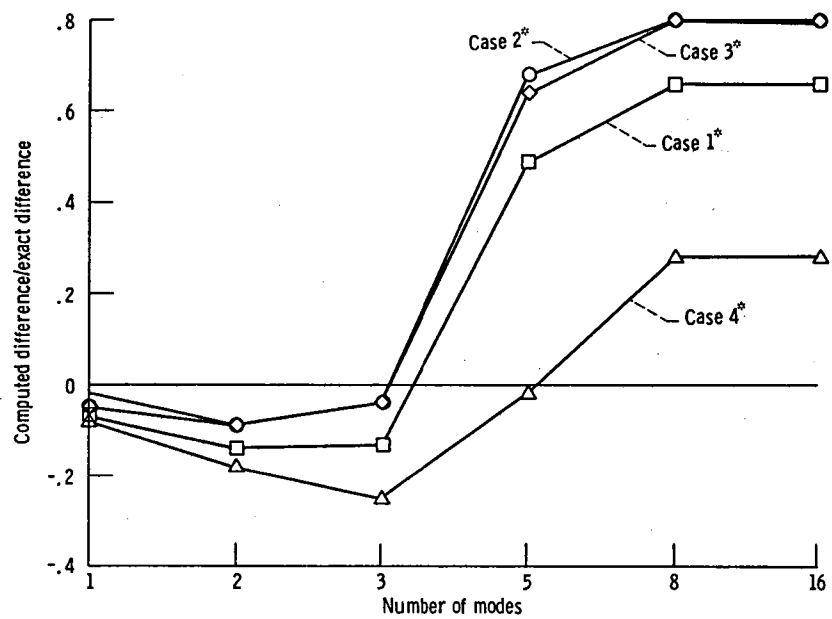


Figure 9. - Stiffness difference at concentrated spring location (sample problem one).
 (* See table I for case definition.)

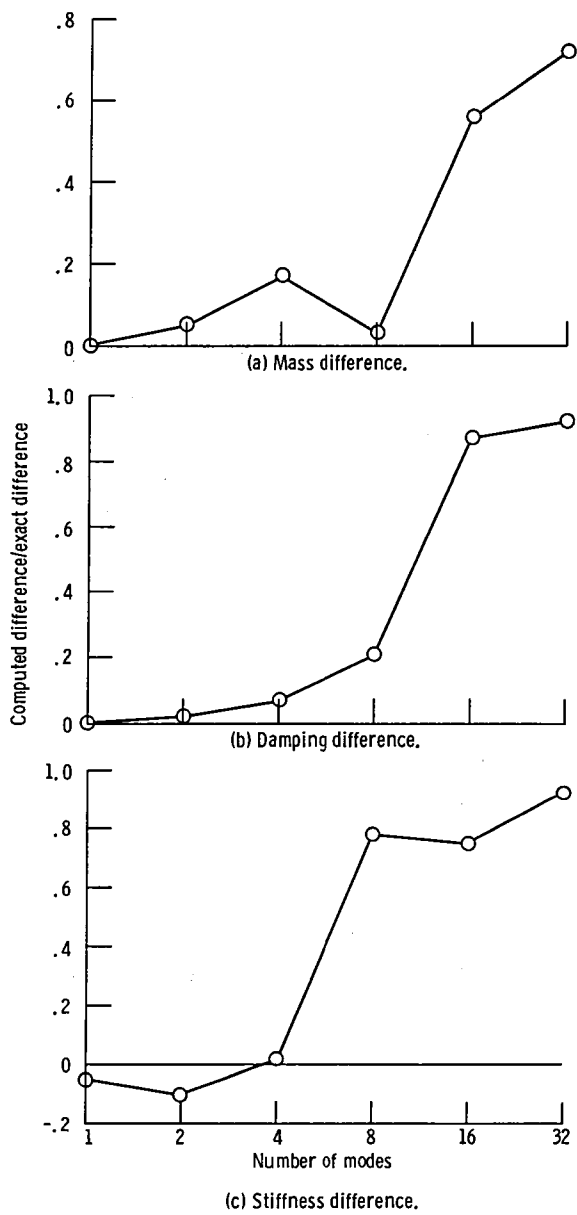
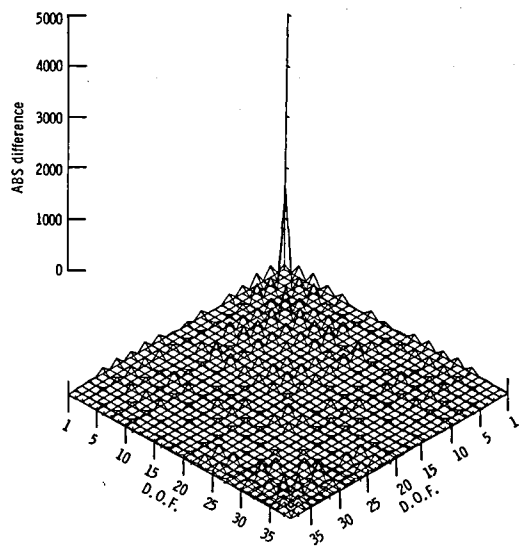
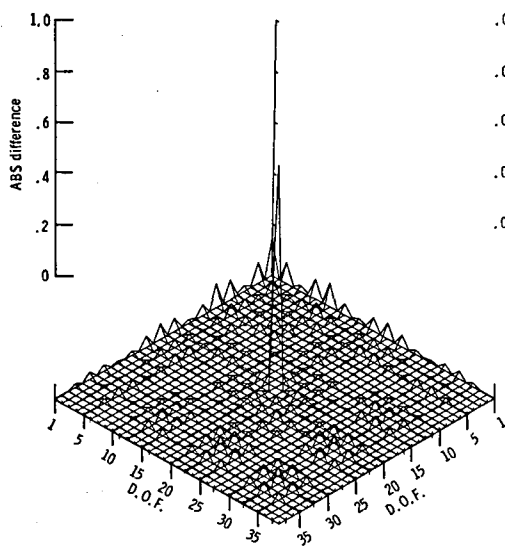


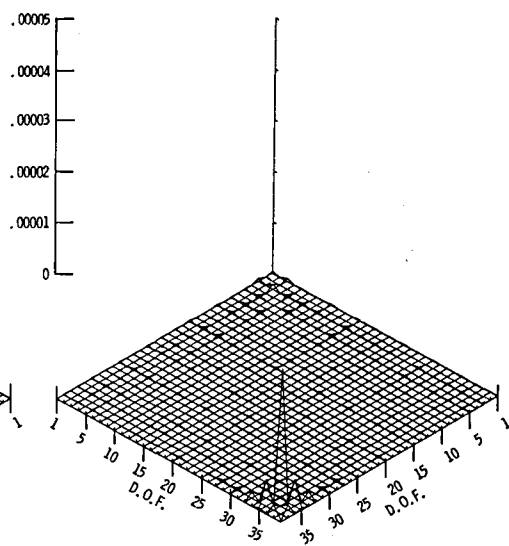
Figure 10. - Computed differences for 32 D.O.F. model.



(a) Stiffness matrix difference.



(b) Damping difference matrix.



(c) Mass difference matrix.

Figure 11. - Computed differences for 32 D.O.F. model, using 16 modes.

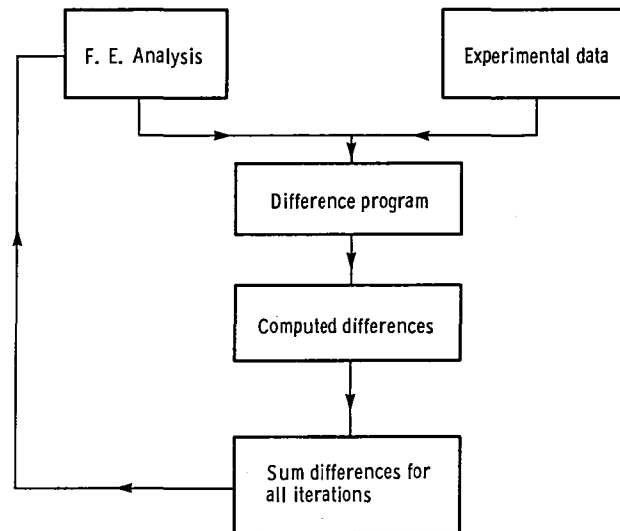


Figure 12. - Iteration scheme.

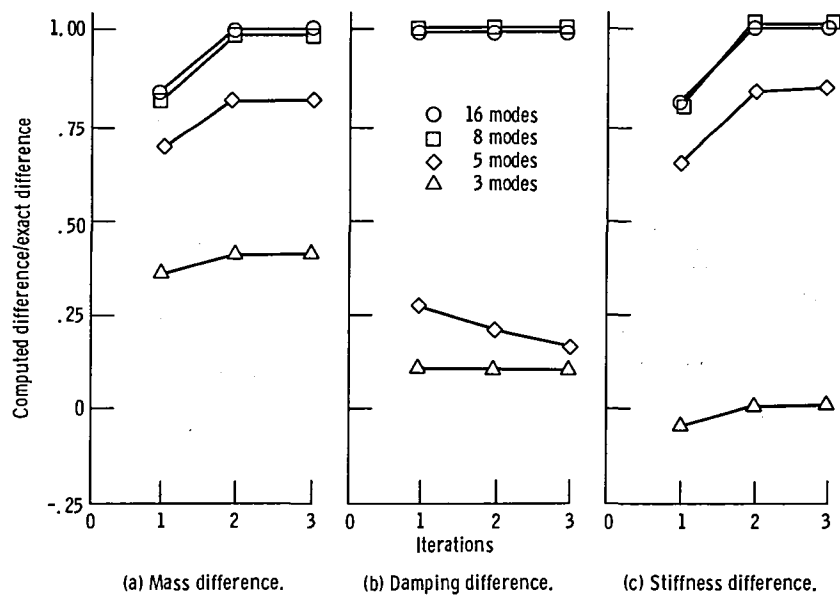
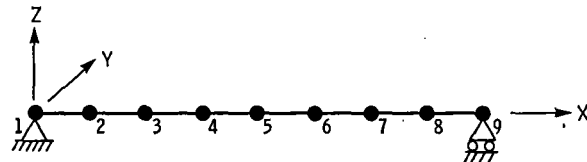
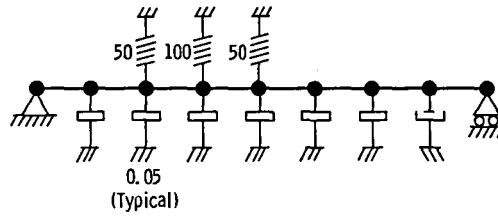


Figure 13. - Improvement in computed differences with iterations (sample problem one, case 3).

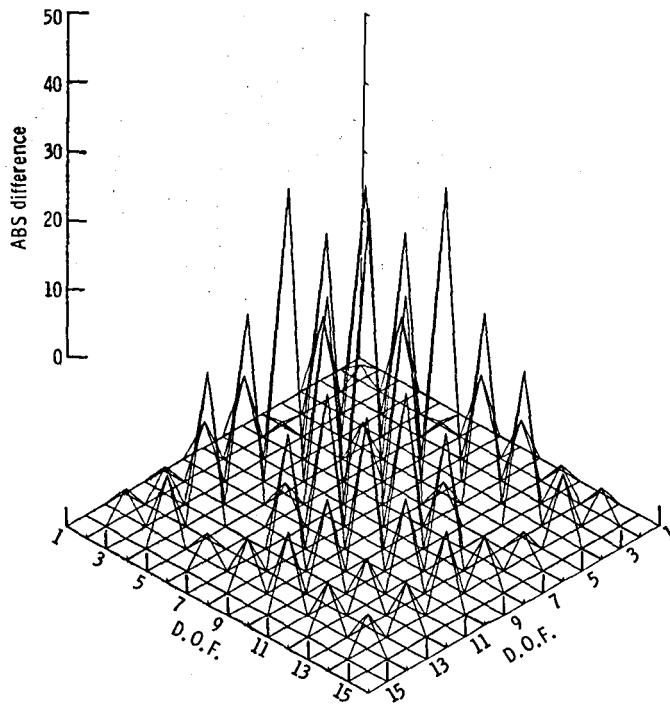


(a) Analytical model.

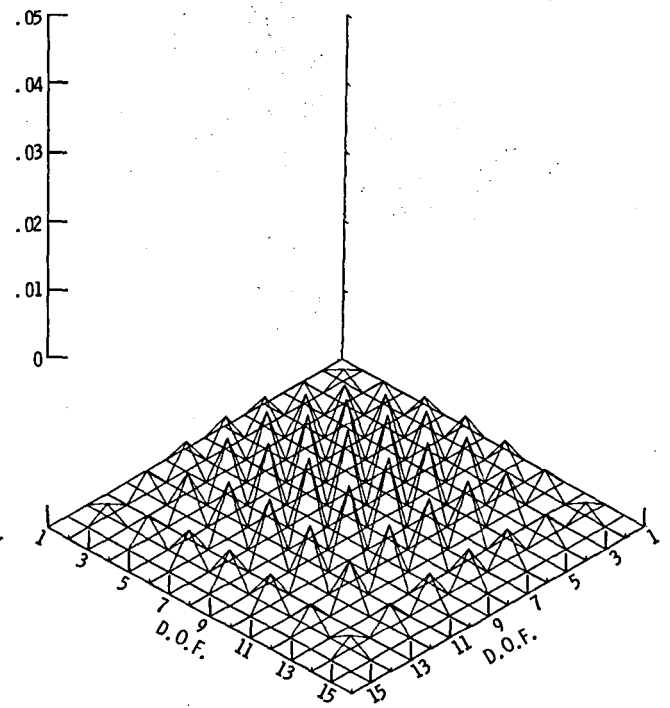


(b) "Experimental" model.

Figure 14. - Sample problem two.

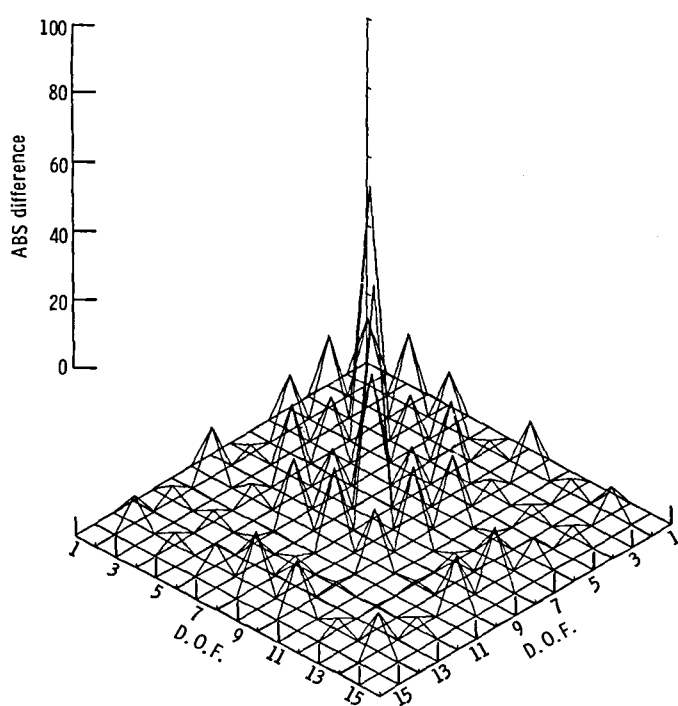


(a) Stiffness difference matrix.

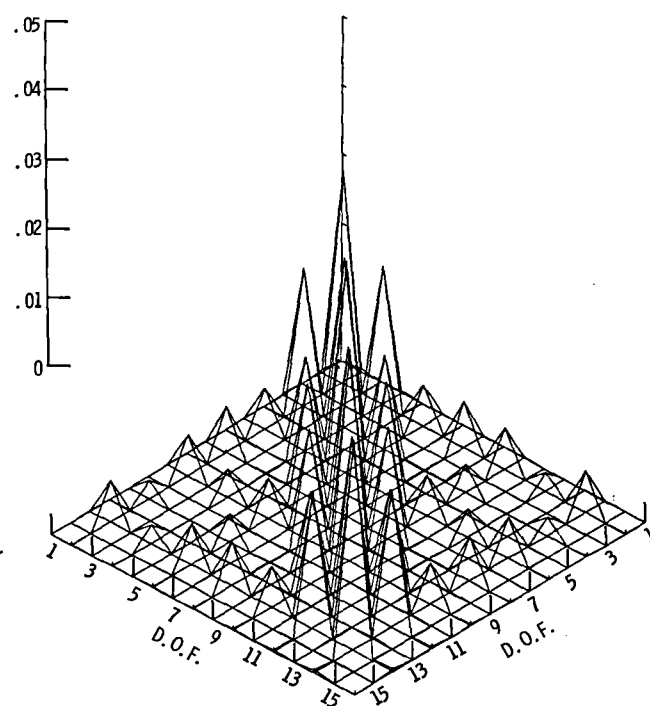


(b) Damping difference matrix.

Figure 15. - Computed differences for sample problem two, using 1 mode.

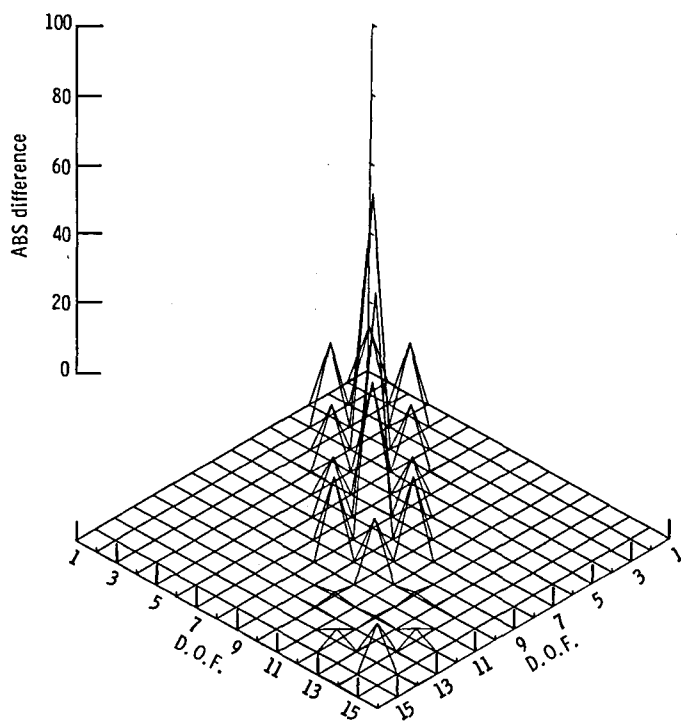


(a) Stiffness difference matrix.

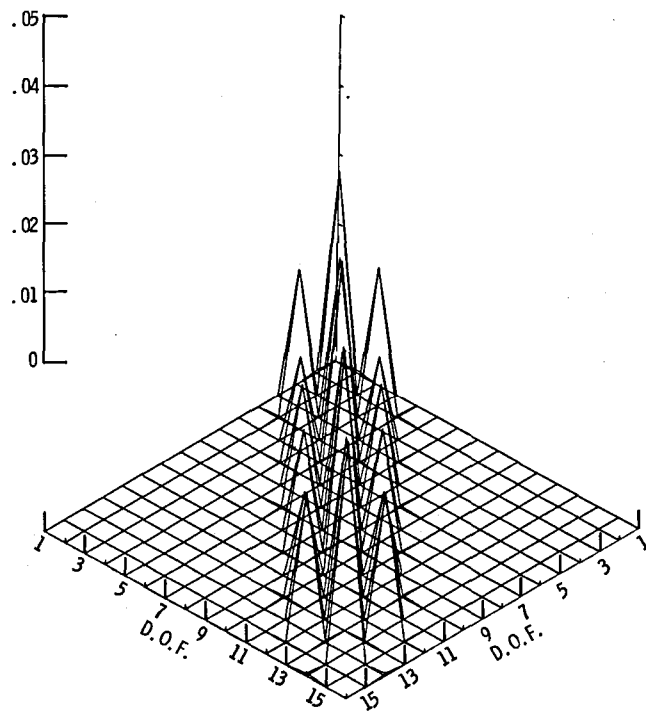


(b) Damping difference matrix.

Figure 16. - Computed differences for sample problem two, using 4 modes.

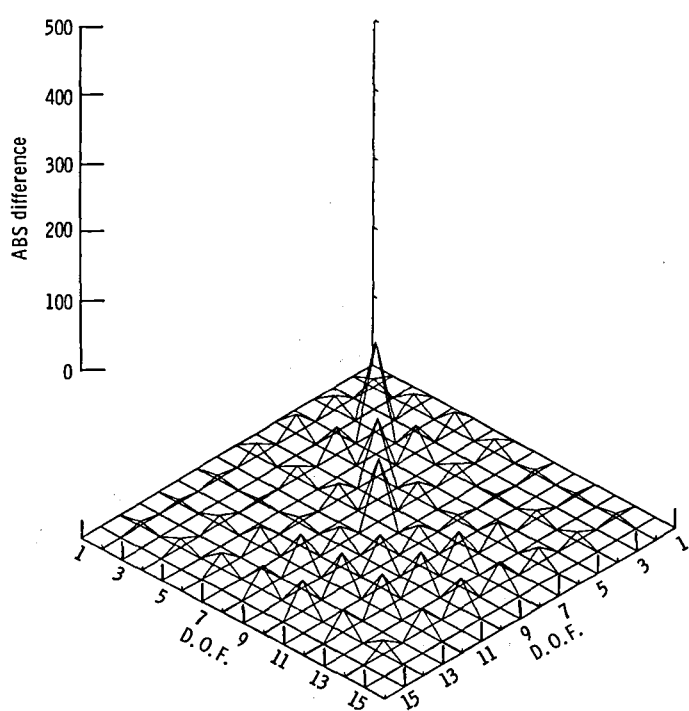


(a) Stiffness difference matrix.

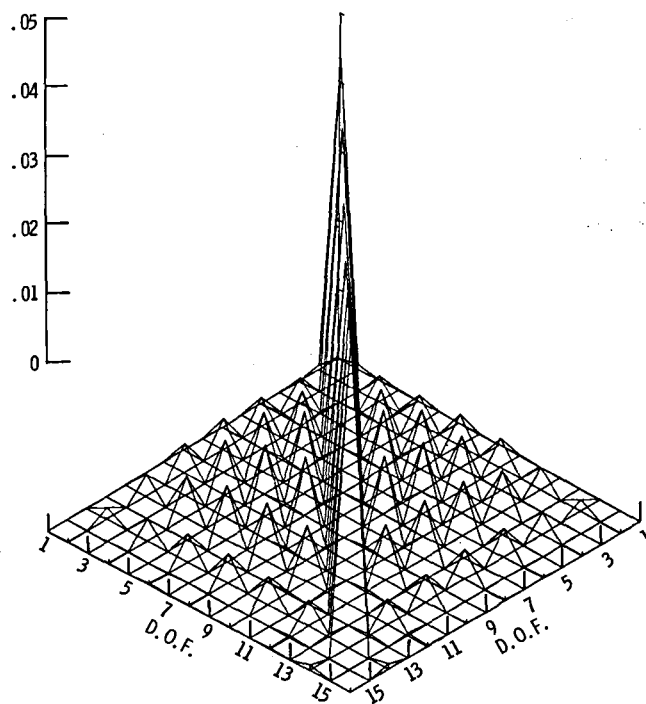


(b) Damping difference matrix.

Figure 17. - Computed differences for sample problem two, using 4 modes and coupling constraints.

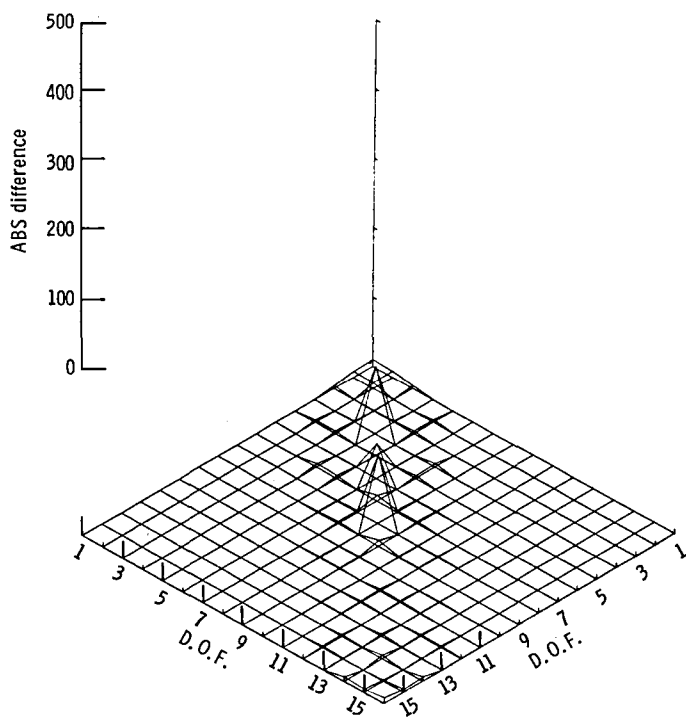


(a) Stiffness difference matrix.

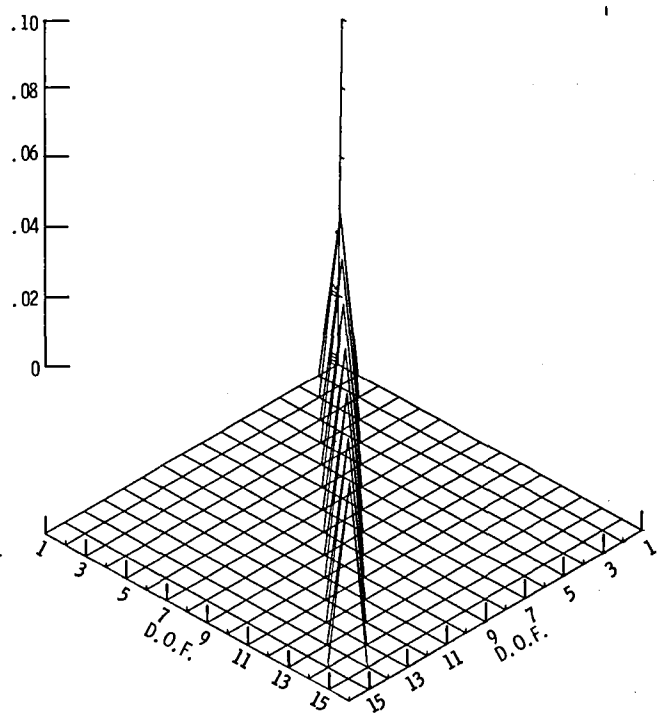


(b) Damping difference matrix.

Figure 18. - Computed differences for sample problem two, using 6 modes.



(a) Stiffness difference matrix.



(b) Damping difference matrix.

Figure 19. - Computed differences for sample problem two, using 16 modes.

1. Report No. NASA TM-87336		2. Government Accession No.		3. Recipient's Catalog No.	
4. Title and Subtitle Identification of Differences Between Finite Element Analysis and Experimental Vibration Data				5. Report Date June 1986	
				6. Performing Organization Code 505-33-7B	
7. Author(s) Charles Lawrence				8. Performing Organization Report No. E-3082	
				10. Work Unit No.	
9. Performing Organization Name and Address National Aeronautics and Space Administration Lewis Research Center Cleveland, Ohio 44135				11. Contract or Grant No.	
				13. Type of Report and Period Covered Technical Memorandum	
12. Sponsoring Agency Name and Address National Aeronautics and Space Administration Washington, D.C. 20546				14. Sponsoring Agency Code	
15. Supplementary Notes					
16. Abstract An important problem that has emerged from combined analytical/experimental investigations is the task of identifying and quantifying the differences between results predicted by F.E. analysis and results obtained from experiment. The objective of this study is to extend and evaluate the procedure developed by Sidhu for correlation of linear F.E. and modal test data to include structures with viscous damping. The desirability of developing this procedure is that the differences are identified in terms of physical mass, damping, and stiffness parameters instead of in terms of frequencies and modes shapes. Since the differences are computed in terms of physical parameters, locations of modeling problems can be directly identified in the F.E. model. From simulated data it was determined that the accuracy of the computed differences increases as the number of experimentally measured modes included in the calculations is increased. When the number of experimental modes is at least equal to the number of translational degrees of freedom in the F.E. model both the location and magnitude of the differences can be computed very accurately. When the number of modes is less than this amount the location of the differences may be determined even though their magnitudes will be under estimated.					
17. Key Words (Suggested by Author(s)) System identification; Structural dynamics; Experimental verification			18. Distribution Statement Unclassified - unlimited STAR Category 39		
19. Security Classif. (of this report) Unclassified		20. Security Classif. (of this page) Unclassified		21. No. of pages	
				22. Price*	

End of Document